

## A SIMPLER METHOD FOR SR INTERFEROMETER CALIBRATION

J.W. Flanagan, H. Fukuma, S. Hiramatsu, H. Ikeda, T. Mitsuhashi, KEK, Tsukuba, Japan

### Abstract

SR interferometers are used for transverse beam size measurement at KEKB. Previous methods of performing absolute calibration of the SR interferometers are very time-consuming, and require dedicated machine time to take the necessary data. We report on a new, simpler method we have developed, wherein we create small local bumps at the SR source point and observe the resulting shifts in the phase of the interference fringes. From these data we can perform an absolute calibration of the system, including the effects of mirror distortion.

### INTRODUCTION

Methods which have been used at KEKB for the absolute calibration of the SR interferometers include measuring mirror distortion with a pinhole mask[1], virtual beam broadening via local bumps[2], physical beam broadening via dispersion bumps[3]. These methods all require dedicated machine time, during which the beam size monitor cannot be used for luminosity tuning. Some of the methods are also quite time-consuming, requiring hours of machine time to take the required data. We present here a new method which of absolute calibration, for which the required data can be taken in a very small amount of time (tens of minutes), and can in principle be taken in parallel with physics running, without stopping the beam-size measurement system or interfering with its use for luminosity tuning. By taking the calibration data at different beam currents and correlating the magnification at each current with the appropriate interference pattern fit parameters, we can also obtain the parameters needed for real-time mirror distortion correction.[1].

### PRINCIPLE OF CALIBRATION

If the light intensities at both slits are the same (though equal light intensities are not a requirement for this method), the interference pattern has the form:

$$y(x) = I_0 \left[ \frac{\sin\left(\frac{2\pi}{\lambda} \frac{w}{f} x + \phi\right)}{\frac{2\pi}{\lambda} \frac{w}{f} x + \phi} \right]^2 \left( 1 + \gamma \cos\left(\frac{2\pi}{\lambda} \frac{D}{f} x + \psi\right) \right),$$

where  $I_0$  is the light intensity through the slits,  $D$  is the separation between the double slits,  $w$  is the slit width,  $f$  is the distance between the secondary principal point of the lens and the camera CCD plane, and  $\lambda$  is the wavelength of light used.  $\phi$  and  $\psi$  are phase offsets depending on the position of the beam off-axis from the slit-camera system.

Now let us examine the dependence of  $\psi$  on the position of the beam. The path length difference between the two

paths through the slits, from the beam to the center of the camera CCD plane, is given by  $\Delta l = (a - c) + (b - d)$ , where  $a, b, c$  and  $d$  are the path lengths shown in Figure 1.

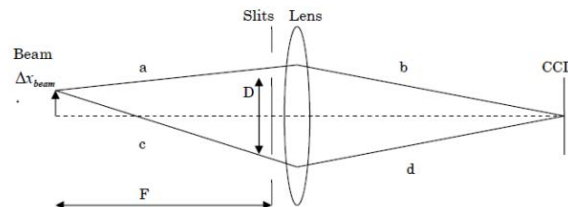


Figure 1: Path lengths from beam to camera.

The path components  $b$  and  $d$  do not change, so for a beam displacement  $\Delta x_{beam}$ ,  $\Delta l = a - c$ , or:

$$\Delta l = \sqrt{F^2 + \left(\frac{D}{2} - \Delta x_{beam}\right)^2} - \sqrt{F^2 + \left(\frac{D}{2} + \Delta x_{beam}\right)^2},$$

where  $F$  is the distance from the beam to the double slits. Since  $D$  and  $\Delta x_{beam}$  are both much smaller than  $F$ , this can be expanded as:

$$\begin{aligned} \frac{\Delta l}{F} &\approx \left[ 1 + \frac{1}{2} \left( \frac{\frac{D}{2} - \Delta x_{beam}}{F} \right)^2 \right] - \left[ 1 + \frac{1}{2} \left( \frac{\frac{D}{2} + \Delta x_{beam}}{F} \right)^2 \right] \\ &\Rightarrow \Delta l \approx \frac{D}{F} \Delta x_{beam}. \end{aligned}$$

Now, the change in phase of the cosine term at the CCD plane,  $\Delta\psi$  (in radians) is given by

$$\Delta\psi = 2\pi \frac{\Delta l}{\lambda},$$

so,

$$\Delta\psi = \frac{2\pi D}{\lambda F} \Delta x_{beam}.$$

Thus, by changing the beam position by a known amount  $\Delta x_{beam}$ , and observing the change in phase of the cosine term in the interferogram, and knowing the wavelength  $\lambda$ , we can calculate the quantity  $\frac{D}{F}$ , which can then be used to calculate the beam size according to:

$$\sigma_{beam} = \frac{\lambda F}{\pi D} \sqrt{\frac{1}{2} \ln \frac{1}{\gamma}}$$

for an assumed-Gaussian beam profile.

The procedure is as follows:

- 1) Create a local bump at the SR source point of height  $\Delta x_{beam}$ ;
- 2) Measure the shift in the cosine fringes of the interference pattern,  $\Delta p$ ;
- 3) Since  $\Delta\psi = 2\pi\Delta p/T$ , where T is the cosine period, then calculate

$$\frac{D}{F} = -\frac{\Delta p}{T} \frac{\lambda}{\Delta x_{beam}}$$

Using typical KEKB parameters,  $\lambda = 500$  nm,  $D = 40$  mm,  $F = 40$  m, a 1-mm  $\Delta x$  gives a  $\Delta\psi$  of about 13 radians, or two complete cosine periods. To avoid changing significantly the shape of the mirror due to changing where the light hits it, it is better to keep the local bump height well below 1 mm. To this end, a series of bumps between  $\pm 0.125$  mm gives a range of  $\Delta\psi$  of up to  $\pm\pi/2$ , which is easily measured. The BPMs have an accuracy of 2-3  $\mu\text{m}$ , which is much smaller than the bump size range. (The above is for the vertical interferometers. For the horizontal ones, where D is 13 mm, a  $\Delta\psi$  of  $\pm\pi/2$  requires bumps of  $\pm 0.4$  mm.)

Measuring  $\frac{D}{F}$  in this way eliminates the need to measure  $D$  and  $F$  separately. This method does not depend on the beam size, and can be performed in parallel with physics running without stopping the interferometer, so there is minimal adverse effect on collision tuning, which is very sensitive to beam size.

In the current system at KEKB, where we have the CCD slightly offset from the focal point of the lens, the above measurements can be conducted at different beam currents (mirror distortions), and the resulting values of  $\frac{D}{F}$  plotted against certain of the interference pattern fit parameters (separation of the sinc terms) to give a calibration curve that can be used for the real-time correction of changes in magnification (or effective  $\frac{D}{F}$ ) due to mirror heating distortions.[1]. These data can also in principle be taken in parallel with physics operation, though to measure over a range of mirror distortions it is necessary to take data over a range of beam currents.

Note: with a variable slit separation, this method could also be used to map part of the surface of the mirror.

## PRELIMINARY EXPERIMENT

Preliminary calibration data were taken in both the horizontal and vertical directions at the KEKB LER. A series of local orbit bumps were created at the SR source point; the horizontal and vertical bump heights are shown in Figures 2 and 3, respectively. The height of the bump is measured by using the values of the two BPMs on either side of the source point:

$$\Delta x_{beam} = \Delta x_{BPM1} \frac{d_{2s}}{d_{1s} + d_{2s}} + \Delta x_{BPM2} \frac{d_{1s}}{d_{1s} + d_{2s}},$$

where  $d_{1s}$  is the distance between the SR source point and BPM 1, and  $d_{2s}$  is the distance between the SR source point

and BPM 2, and  $\Delta x_{BPM1}$  and  $\Delta x_{BPM2}$  are the changes in the closed orbit at BPMs 1 and 2, respectively.

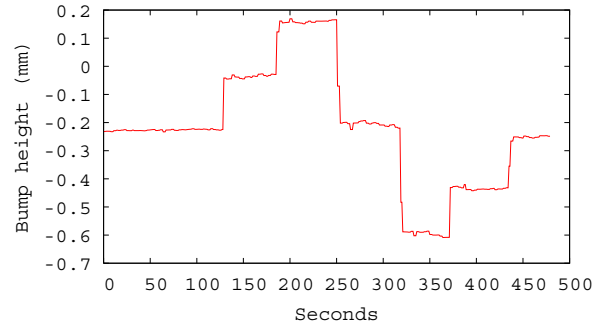


Figure 2: Horizontal bump height as function of time.

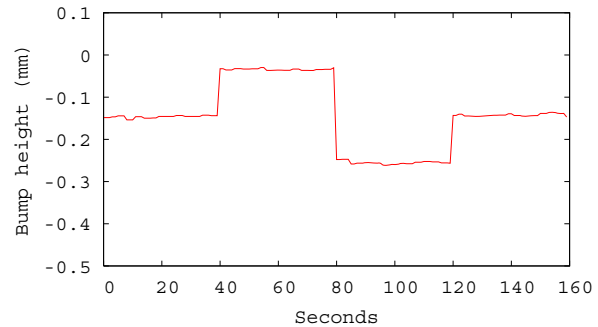


Figure 3: Vertical bump height as function of time.

The data can be taken in a few minutes, as seen from the time scales. Indeed, due to orbit drift, it is important to take the data as quickly as possible, particularly in the vertical direction. The reason for this is that as the beam moves around, the location of the SR fan on the the extraction mirror changes, which changes the shape of the mirror due to heat distortion. This effect is not noticeable in the horizontal direction, because we have horizontal bending magnets as our source magnets, so the distribution of SR on the mirror does not change appreciably as the beam moves. In the vertical direction, however, due to the vertical narrowness of the fan, the change in the shape of the mirror as the beam moves cannot be ignored. The change in the curvature of the mirror both changes the magnification of the mirror from the steady state value that one is trying to measure, and also introduces extraneous shifts in the phase of the cosine term as a function of bump height, which skew the calibration. To minimize this effect, the vertical bump is “tilted”; as the beam moves off-axis, the orbit is also angled so that the location where the SR fan hits the mirror is kept constant. This is accomplished by creating a local bump defined by:

$$\Delta y_{BPM1} = \Delta y_{beam} \frac{d_{m1}}{d_{ms}},$$

and

$$\Delta y_{BPM_2} = \Delta y_{beam} \frac{d_{m2}}{d_{ms}},$$

where  $d_{m1}$  is the distance between the extraction mirror and BPM 1,  $d_2$  is the distance between the extraction mirror and BPM 2, and  $d_{ms}$  is the distance from the extraction mirror and the SR source point. An example of a tilted bump is shown in Figure 4.

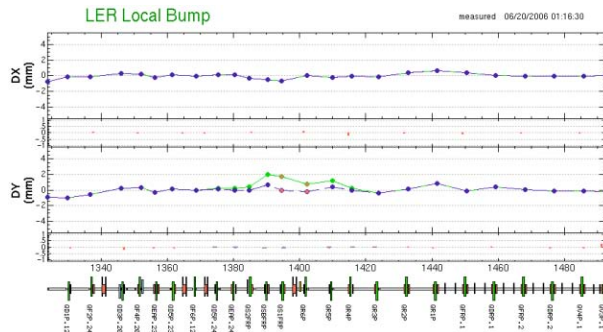


Figure 4: Example of a “tilted” closed orbit bump in the vertical direction. Note: height of bump illustrated is 10 times larger than that used for SR monitor calibration.

The difference between the BPMs on either side of the source point is monitored in addition to the bump height. The location of the mirror spot  $\Delta y_{mirror}$  is calculated as:

$$\Delta y_{mirror} = (\Delta y_{BPM_2} - \Delta y_{BPM_1}) \frac{d_{m2}}{d_{12}} + \Delta y_{BPM_2},$$

where  $d_{12}$  is the distance between BPM 1 and BPM 2. To ensure that the data were taken when the beam orbit is stable in position and angle at the SR source point, only data during which both  $\Delta y_{beam}$  and  $\Delta y_{mirror}$  are constant are used.

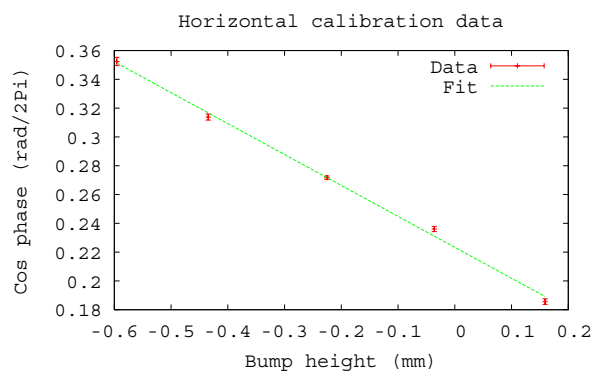


Figure 5: Horizontal cosine-term phase as a function of closed-orbit bump height.

The phase of the cosine term is plotted as a function of bump height in Figures 5 and 6. From the linear fits shown in these plots, the ratio  $\frac{D}{F}$  can be calculated and compared to the results of calibration by pinhole mask. In the horizontal direction,  $\frac{D}{F} = 1.08 \times 10^{-4} \pm 0.04 \times 10^{-4}$  (fitting error), which is within  $\sim 1\sigma$  away from the value of

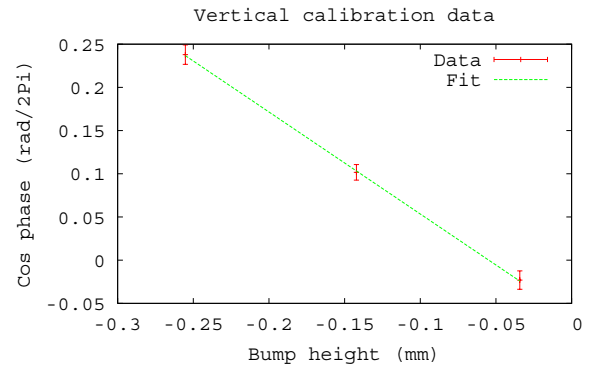


Figure 6: Vertical cosine-term phase as a function of closed-orbit bump height.

$1.05 \times 10^{-4} \pm 0.03 \times 10^{-4}$  derived from calibration via pinhole mask. The corresponding values in the vertical direction are  $5.94 \times 10^{-4} \pm 0.08 \times 10^{-4}$  and  $6.19 \times 10^{-4} \pm 0.02 \times 10^{-4}$  (fitting errors), for the bump calibration and mask calibration, respectively. The vertical bump calibration data were taken at an average beam current of 1553 mA, and the mask calibration data were taken at an average beam current of  $\sim 1540$  mA. Note that the value of  $D/F$  in the vertical direction has an observed dependence on the beam current due to the heat load of the SR fan, whereas the horizontal direction shows no such dependence. The extraction windows and some of the mirrors in the optical beam line have been changed since the pinhole mask calibration was performed, so the calibration may in fact have changed somewhat. Nevertheless, the two methods do give results to within  $\sim 4\%$  of each other.

## SUMMARY

We have presented a new method for calibrating the SR interferometer, which is much simpler and faster than previous methods employed, and requires no additional equipment beyond the interferometer and BPMs, only the ability to move the beam at the SR source point. For a horizontal-bending source magnet, preliminary measurements show that the method gives excellent agreement with pinhole-mask calibration in the horizontal axis, where moving the beam does not change the heat distribution on the surface of the extraction mirror significantly. Care must be taken in the vertical direction when moving the beam that the location on the mirror where the synchrotron radiation fan hits is held constant. This requires a “tilted” local bump in the vertical direction.

## REFERENCES

- [1] M. Arinaga *et al.*, NIM, A499, p. 100 (2003).
- [2] J.W. Flanagan *et al.*, Proc. 14th Symposium on Accel. Science and Technology (SAST 2003), Tsukuba, Japan, p. 440 (2003).
- [3] N. Iida and Y. Funakoshi, private communication.